Electronic Supplementary Information

Discovery of a New Intercalation-Type Anode for High-Performance Sodium Ion Batteries

Yajun Zhao,[a] Tao Sun,[a] Qing Yin,[a] Jian Zhang,[a] Shuoxiao Zhang,[a] Jianeng Luo,[a] Hong Yan,[a] Lirong Zheng,[b] Jingbin Han,*[a] and Min Wei[a]

[a.] *State Key Laboratory of Chemical Resource Engineering, Beijing Advanced Innovation Center for Soft Matter Science and Engineering, Beijing University of Chemical Technology, Beijing 100029, P. R. China.*

[b.] *Institute of High Energy Physics, Chinese Academy of Science, Beijing 100049, P. R. China.*

Author Information

* Corresponding authors:

E-mail: hanjb@mail.buct.edu.cn

Materials characterizations

The morphology of the sample was observed by scanning electron microscope (SEM, Zeiss Supra55) with an accelerating voltage of 20 KV. High-resolution transmission electron microscopy (HRTEM) images were collected by a TECNAI G2 F30 instrument, equipped by an energy dispersive spectroscopy (EDS) to determine the distribution of Co and Fe. X-ray diffraction (XRD) patterns were recorded by a Rigaku D/max-2500B2+/PCX system with Cu Kα radiation (λ = 0.15418 nm) at 40 kV, 30 mA. Cyclic voltammetry was performed on a CHI660 electrochemical workstation (Chenhua Instruments Co., China). All the electrochemical measurements were carried out at room temperature.X-ray photoelectron spectroscopy (XPS, Thermo Electron Corporation ESCALAB 250 XPS spectrometer) were recorded using a twin anode Al Kα X-ray source with a 30 eV pass energy and a 0.5 eV step size. The amount of water was analyzed by thermogravimetry and differential thermal analysis (TG-DTA) in air flow with a heating rate of 10 °C min^{-1}. Elemental analysis was carried out using a Shimadzu ICPS-7500 inductively coupled plasma atomic emission spectroscopy (ICP-AES). Extend X-ray absorption fine structure spectroscopy (EXAFS) for the Co and Fe K-edge was performed at the beamline 1W1B of the Beijing Synchrotron Radiation Facility (BSRF), Institute of High Energy Physics (IHEP), Chinese Academy of Sciences (CAS).

Theoretical calculations

Density functional theory (DFT) calculations were performed using the Vienna Ab-initio Simulation Package (VASP) on a supercell of 2×2×1. The gradient-corrected exchange correlation functional of Perdew-Burke-Ernzerh generalized-gradient-approximation(PBE-GGA) was employed.[1,2] A plane-wave basis with 480 eV energy cutoff was adopted using the

projector augmented wave (PAW) basis-set and the converge criteria of the force on each relaxed atoms below 0.1 eV/Å were used.[3] The convergence criteria were chosen such that the changes were 10^{-5} eV for the energy. The vacuum region between slabs was 15 Å. A climbing image-nudged elastic band (CI-NEB) method was used to study the diffusion state using the 5×5×1 k-point sampling.[4,5] The calculation on diffusion barrier of Na was performed on two models of CoFe-LDH with interlayer spacing of 0.75 and 0.80 nm to simulated CO_3^{2-} and NO_3^- pillared LDH, respectively. To reduce the complexity of the calculation, the pre-existing interlayer species were omitted.

Supplementary Figures

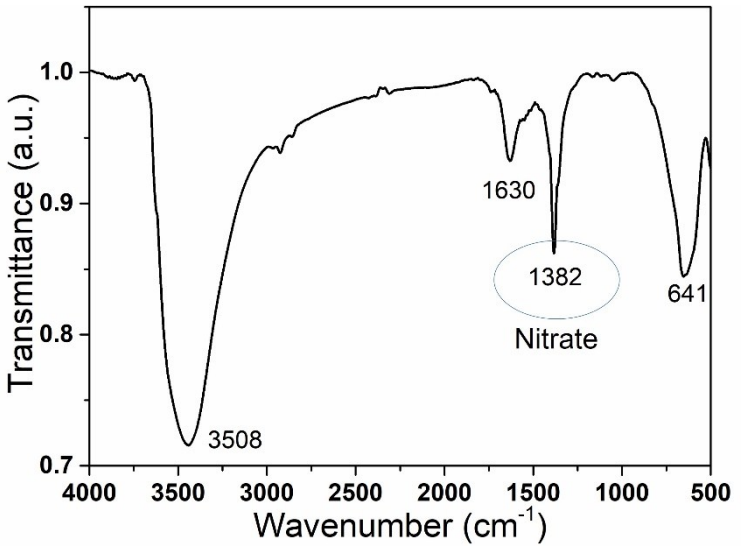

Fig. S1 (a) FT-IR spectrum of nitrate-pillared CoFe-LDH.

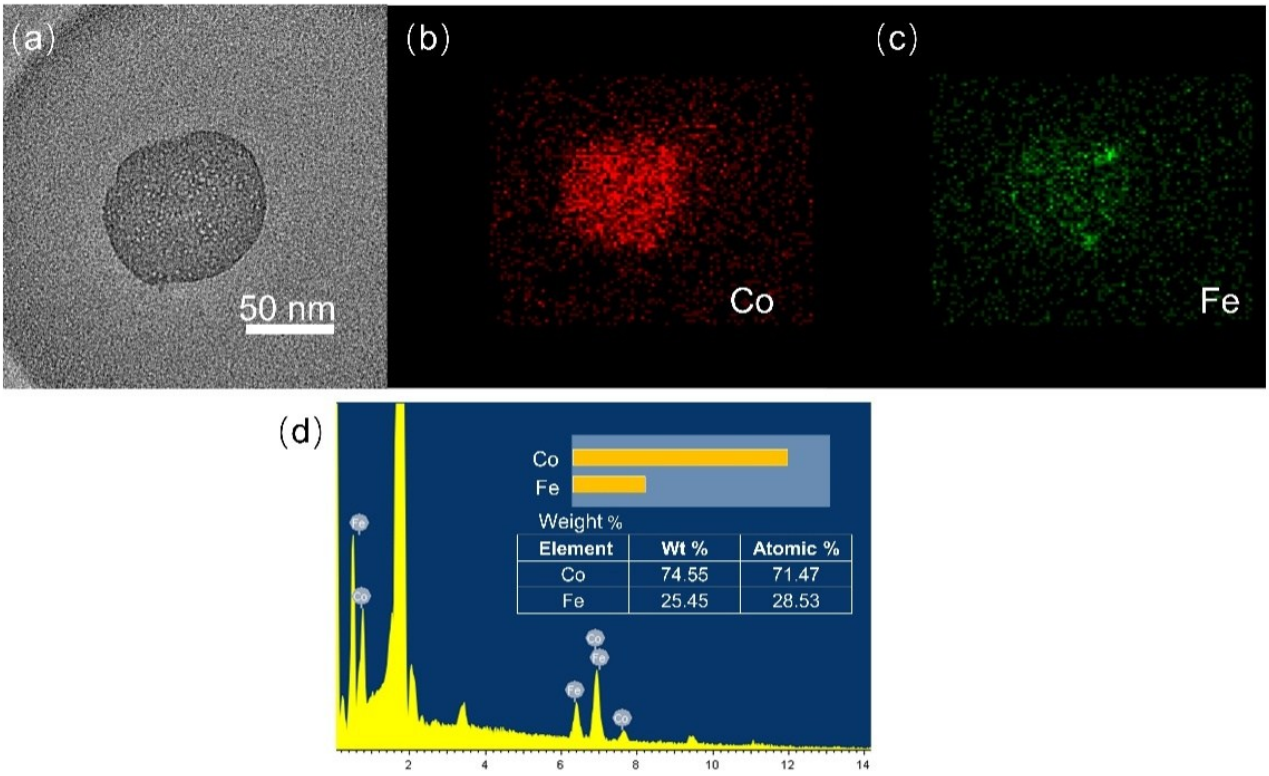

Fig. S2 (a) HRTEM image and (b and c) elemental mapping images of an individual CoFe-NO_3^--LDH nanoplatelet. (d) EDX spectrum of the CoFe-NO_3^--LDH.

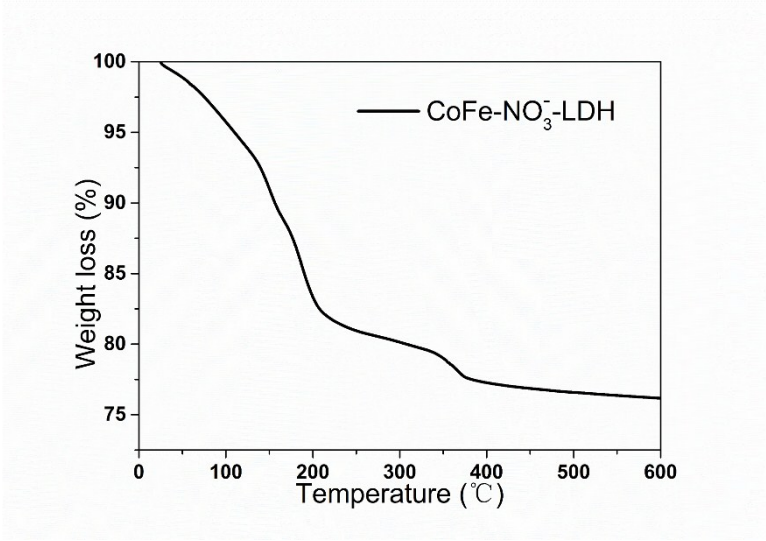

Fig. S3 TG curve of the CoFe-NO_3^--LDH.

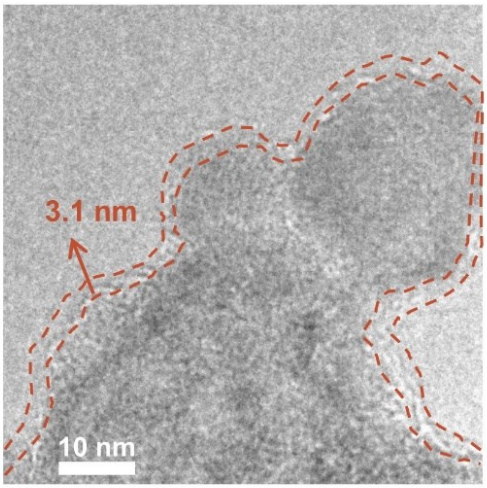

Fig. S4 HR-TEM image of SEI film on the surface of CoFe-NO_3^--LDH nanoplatelet after 1 cycle of charge-discharge.

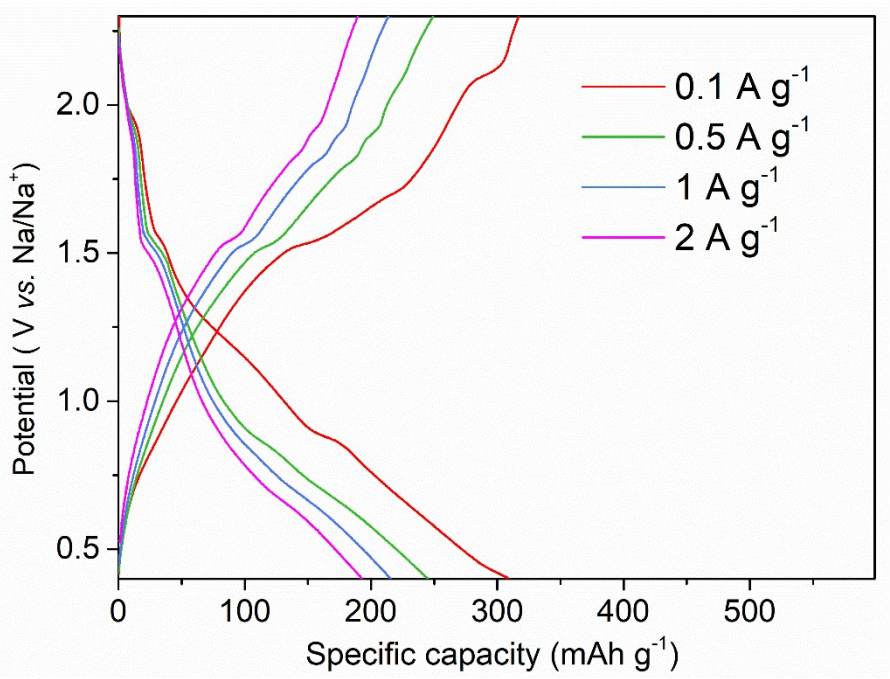

Fig. S5 Galvanostatic charge/discharge curves of CoFe-NO_3^--LDH at various current densities.

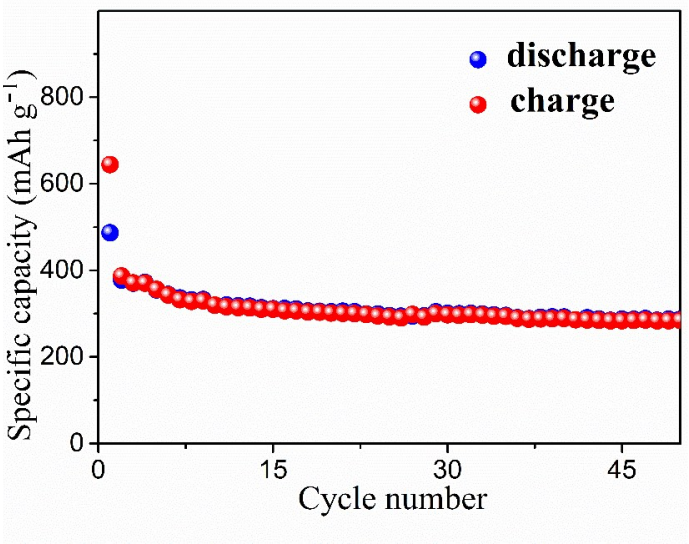

Fig. S6 The cycling performance of CoFe-NO_3^--LDH at 100 mA g^{-1}.

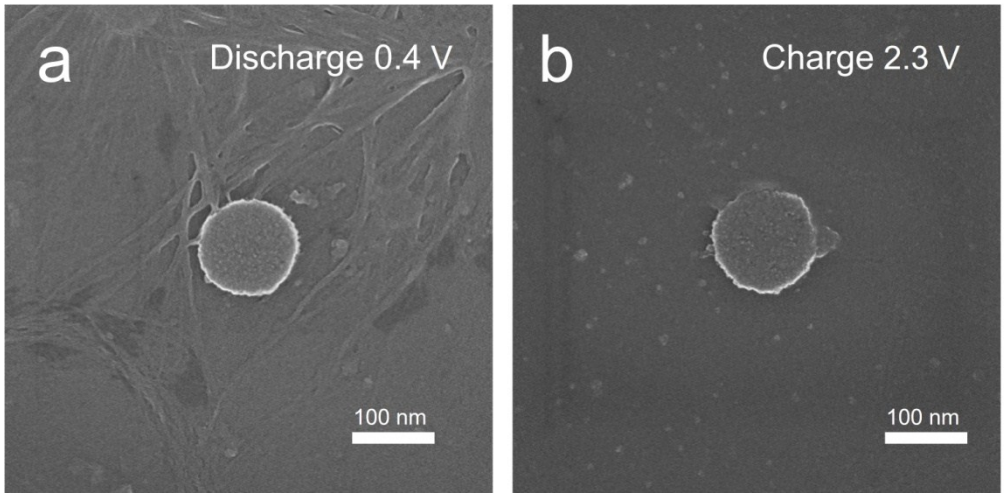

Fig. S7 SEM image of CoFe-NO_3^--LDH electrodes coated by acetylene black after discharging to 0.4 V (a) and charging to 2.3 V (b).

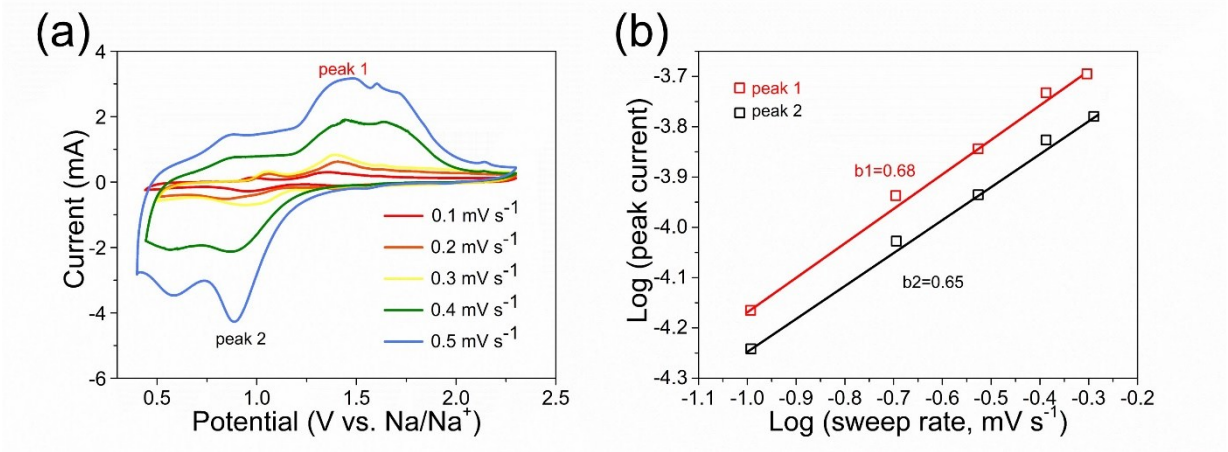

Fig. S8 (a) Cyclic voltammograms of the CoFe-NO_3^--LDH electrode at various scan rates. (b) Determination of the *b* value using the relationship between peak current and scan rate.

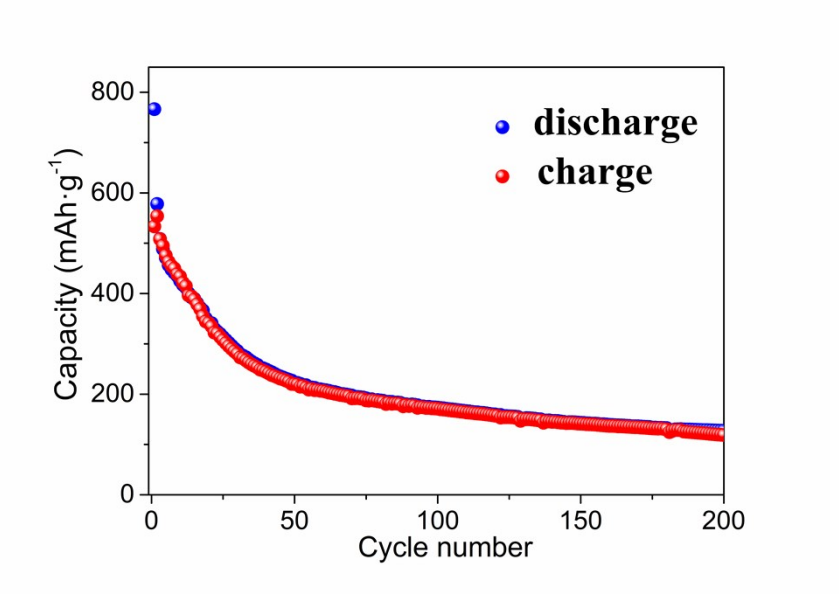

Fig. S9 Cycling performance of CoFe-NO_3^--LDH electrode at a current density of 1 A g^{-1} with a voltage window 0.01 V to 3 V.

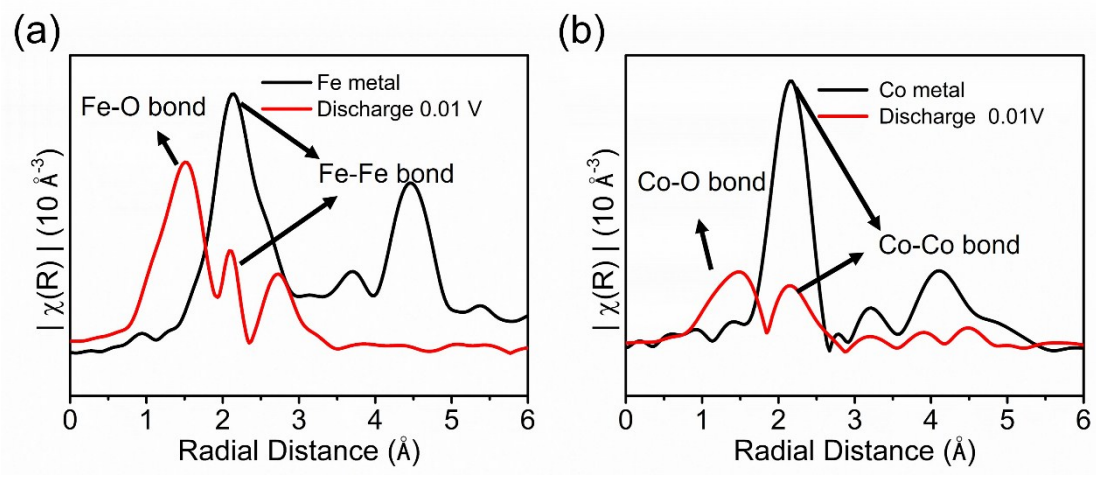

Fig. S10 (a) Fe and (b) Co edge FT-EXAFS for pristine CoFe-NO_3^--LDH electrode the electrode after discharging to 0.01 V.

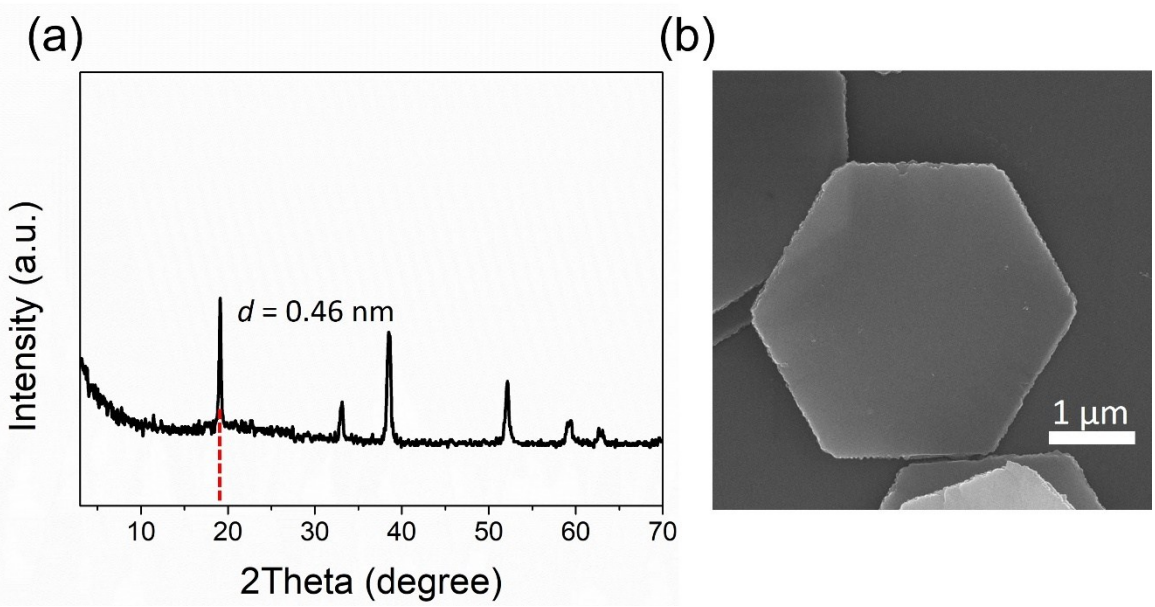

Fig. S11 (a) XRD pattern and (b) SEM image of Co^{2+}/Fe^{2+} hydroxide.

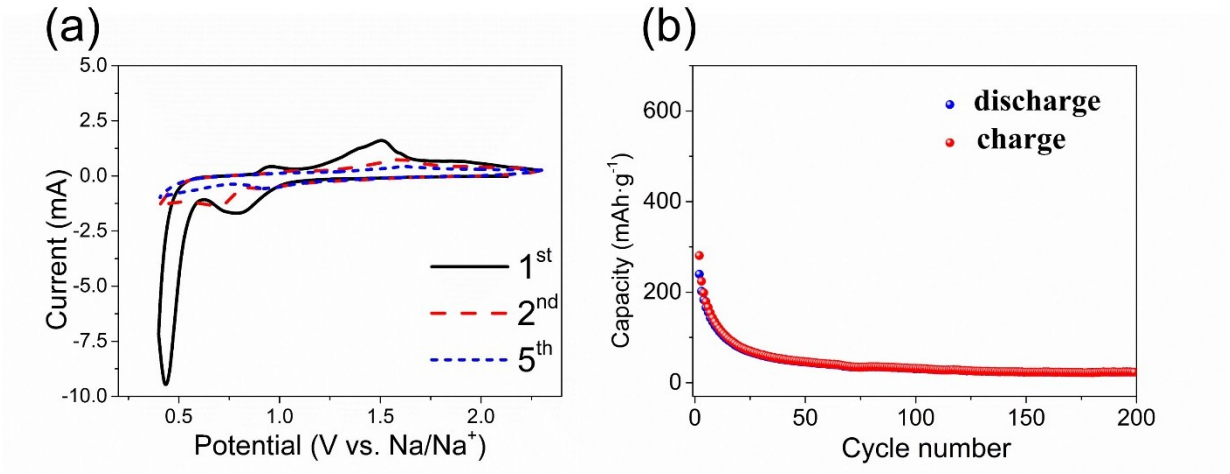

Fig. S12 (a) CV curves of the Co^{2+}/Fe^{2+} hydroxide at 0.2 mV s^{-1}. (b) Cycling performance of Co^{2+}/Fe^{2+} hydroxide electrode tested at 1 A g^{-1}.

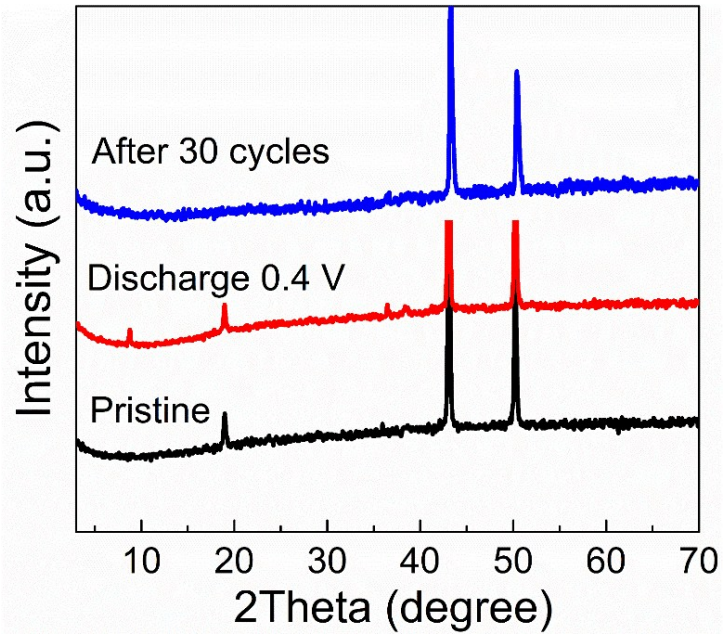

Fig. S13 XRD patterns of the Co^{2+}/Fe^{2+} hydroxide electrodes: pristine (black line), after 1st discharging to 0.4 V (red line) and after 30 charge/discharge cycles (blue line).

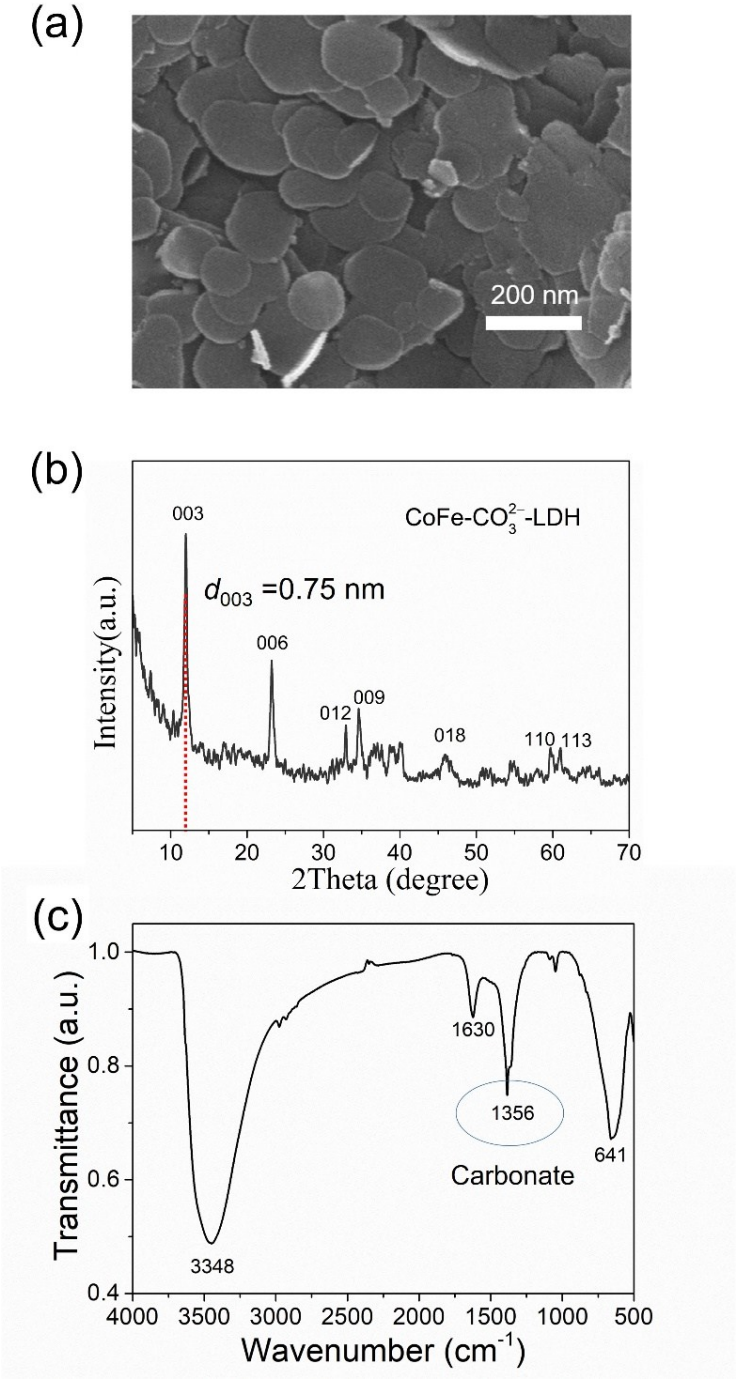

Fig. S14 (a) SEM image, (b) XRD pattern and (c) FT-IR spectrum of CoFe-CO_3^{2-}-LDH.

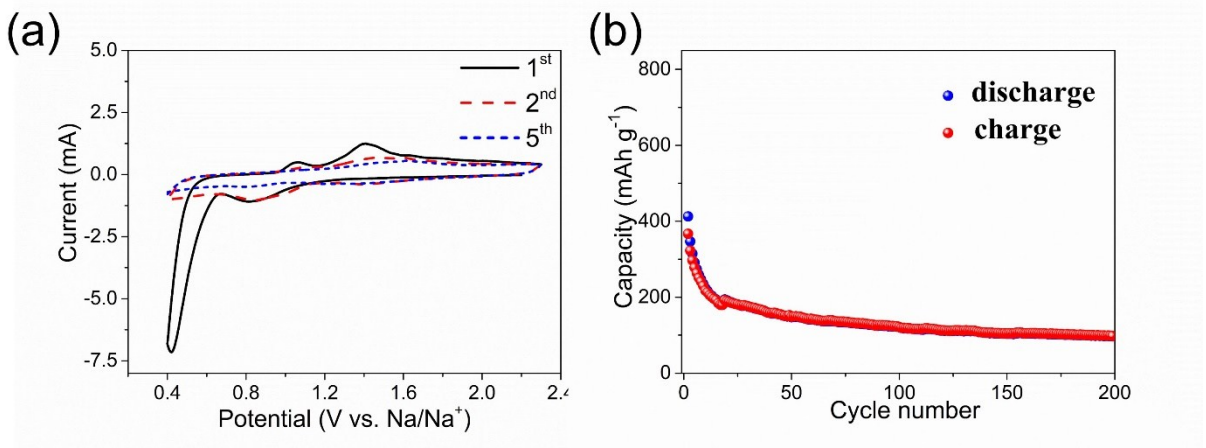

Fig. S15 (a) CV curves at 0.2 mV s^{-1} and (b) cycling performance in 200 cycles at 1 A g^{-1} for CoFe-CO_3^{2-}-LDH electrode.

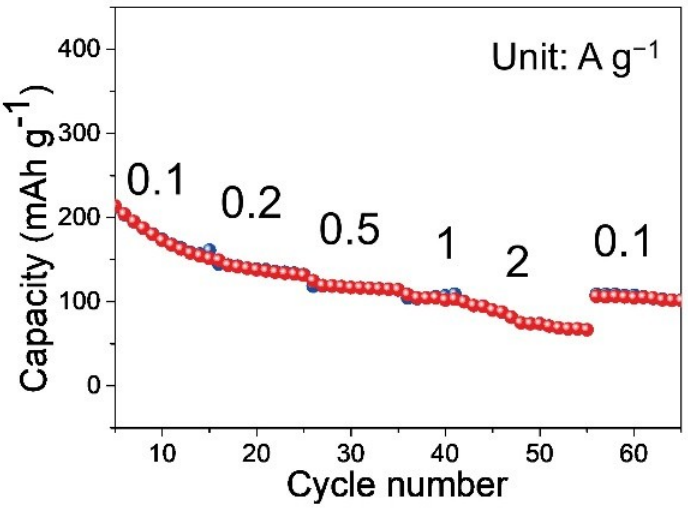

Fig. S16 Rate performance of the CoFe-CO_3^{2-}-LDH.

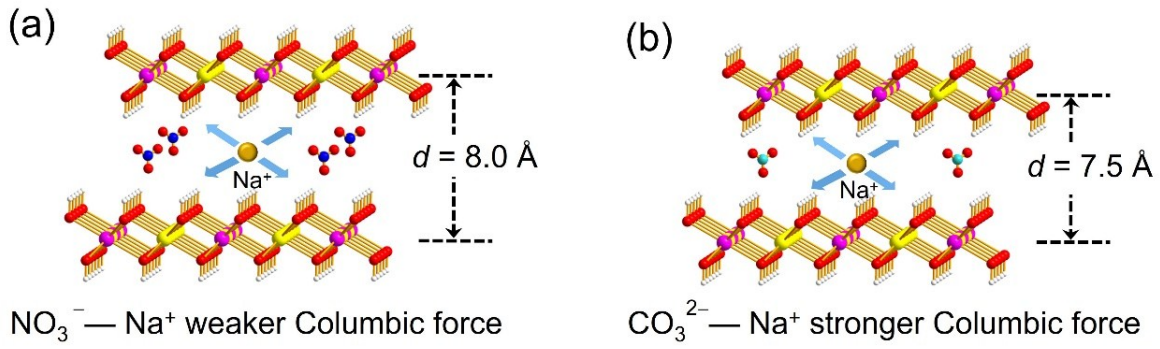

Fig. S17 Schematic illustration of the Na^+ diffusion in (a) CoFe-NO_3^--LDH and (b) CoFe-CO_3^{2-}-LDH with weaker and stronger Columbic force, respectively.

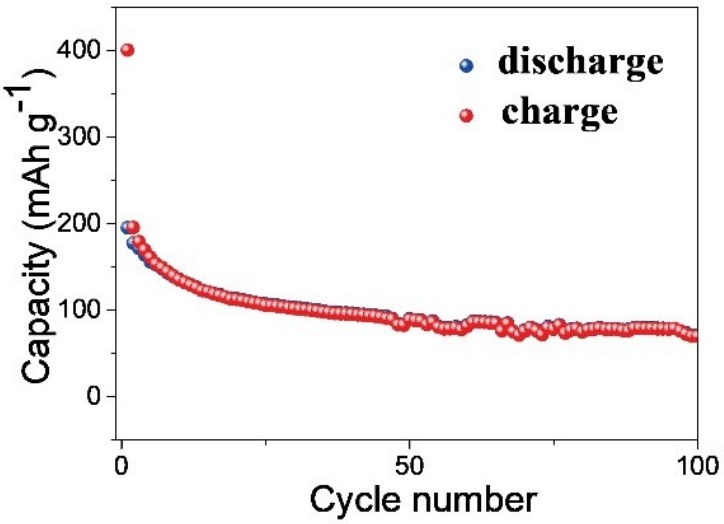

Fig. S18 Cycling performance of CoFe-NO_3^--LDH electrode without lattice water at a current density of 1 A g^{-1} within voltage window of 0.4 to 2.3 V.

Reference

1. J. P. Perdew, K. Burke and M. Ernzerhof, *Phys. Rev. Lett.*, 1996, **77**, 3865−3868.
2. A. D. Becke, *Phys. Rev. A*, 1988, **38**, 3098−3100.
3. P. E. Blöchl, *Phys. Rev. B*, 1994, **50**, 17953−17979.
4. H. J. Monkhorst and J. D. Pack, *Phys. Rev. B*, 1976, **13**, 5188−5192.
5. G. Henkelman, B. P. Uberuaga and H. Jónsson, *J. Chem. Phys.*, 2000, **113**, 9901−9904.